



OPEN

SUBJECT AREAS:
MUSCLE STEM CELLS
CELL GROWTHReceived
5 February 2014Accepted
8 May 2014Published
11 June 2014Correspondence and
requests for materials
should be addressed to
S.K. (kimusige@
kumamoto-u.ac.jp)

Parathyroid hormone and parathyroid hormone type-1 receptor accelerate myocyte differentiation

Shigemi Kimura & Kowasi Yoshioka

Department of Pediatrics, Graduate School of Medical Sciences, Kumamoto University, Kumamoto, Japan.

The ZHTc6-MyoD embryonic stem cell line expresses the myogenic transcriptional factor MyoD under the control of a tetracycline-inducible promoter. Following induction, most of the ZHTc6-MyoD cells differentiate to myotubes. However, a small fraction does not differentiate, instead forming colonies that retain the potential for myocyte differentiation. In our current study, we found that parathyroid hormone type 1 receptor (PTH1R) expression in colony-forming cells at 13 days after differentiation was higher than that in the undifferentiated ZHTc6-MyoD cells. We also found that PTH1R expression was required for myocyte differentiation, and that parathyroid hormone accelerated the differentiation. Our analysis of human and mouse skeletal muscle tissues showed that most cells expressing PTH1R also expressed Pax7 and CD34, which are biomarkers of satellite cells. Furthermore, we found that parathyroid hormone treatment significantly improved muscle weakness in dystrophin-deficient mdx mice. This is the first report indicating that PTH1R and PTH accelerate myocyte differentiation.

Duchenne muscular dystrophy (DMD) is caused by the defective expression of the dystrophin gene, which results in the absence of the dystrophin protein in muscle fibers¹. Novel approaches for the treatment of DMD have shown promise in pre-clinical and/or proof-of-concept clinical studies^{2,3}. However, no clear effective therapy has been identified thus far.

We previously generated the genetically engineered embryonic stem cell (ESC) line ZHTc6-MyoD, which expresses the myogenic transcriptional factor MyoD under the control of a tetracycline-inducible promoter⁴. Although most of the ZHTc6-MyoD cells differentiated to a myocyte lineage after the removal of the tetracycline analog doxycycline (Dox), a small number of cells that continued to express MyoD formed colonies and did not differentiate (Fig. 1a). These colonies were cultured in the maintenance medium as undifferentiated ESCs, and a similar pattern of differentiation to the myocyte lineage was observed following the removal of Dox. In another previous study, C2C12 mouse myoblast cells also demonstrated a similar pattern of differentiation after serum starvation, in which a small fraction of the C2C12 cells, designated as “reserve cells,” remained undifferentiated and retained the potential to differentiate into myotubes⁵.

Satellite cells are mononucleated myogenic cells located between the basement and plasma membranes of muscle fibers⁶. Satellite cells are characterized by positive Pax7 immunoreactivity and the presence of surface receptors including α 7 integrin, β 1 integrin, CD34, NCAM, c-met, and CXCR4^{7–12}. Injury-activated satellite cells have been shown to proliferate and differentiate into myofibers, with some remaining as satellite cells^{13–15}. Thus, the stemness properties of the C2C12 and ZHTc6-MyoD cells are similar to those of satellite cells.

In our current study, we determined that the differentiation of satellite cells to myotubes is accelerated by parathyroid hormone (PTH) and the expression of the parathyroid -1 receptor (PTH1R). We also demonstrated that the administration of PTH significantly improved muscle weakness in dystrophin-deficient mdx mice.

Results

cDNA microarray analysis of ZHTc6-MyoD cells before differentiation and colony-forming cells at 13 days after differentiation. To analyze the difference between undifferentiated ZHTc6-MyoD cells before induction of differentiation and colony-forming cells at 13 days after differentiation of the ZHTc6-MyoD cells, total RNA was isolated and the gene expression profiles were compared using cDNA microarray analysis (Figs. 1b and 1c). The expression of several genes in the colony-forming cells at 13 days after differentiation was greater than that in undifferentiated ZHTc6-MyoD cells. MyoD expression in the colony-forming cells at 13 days after differentiation was 90 times that in the undifferentiated ZHTc6-MyoD cells, whereas Pax7 and dystrophin expression was

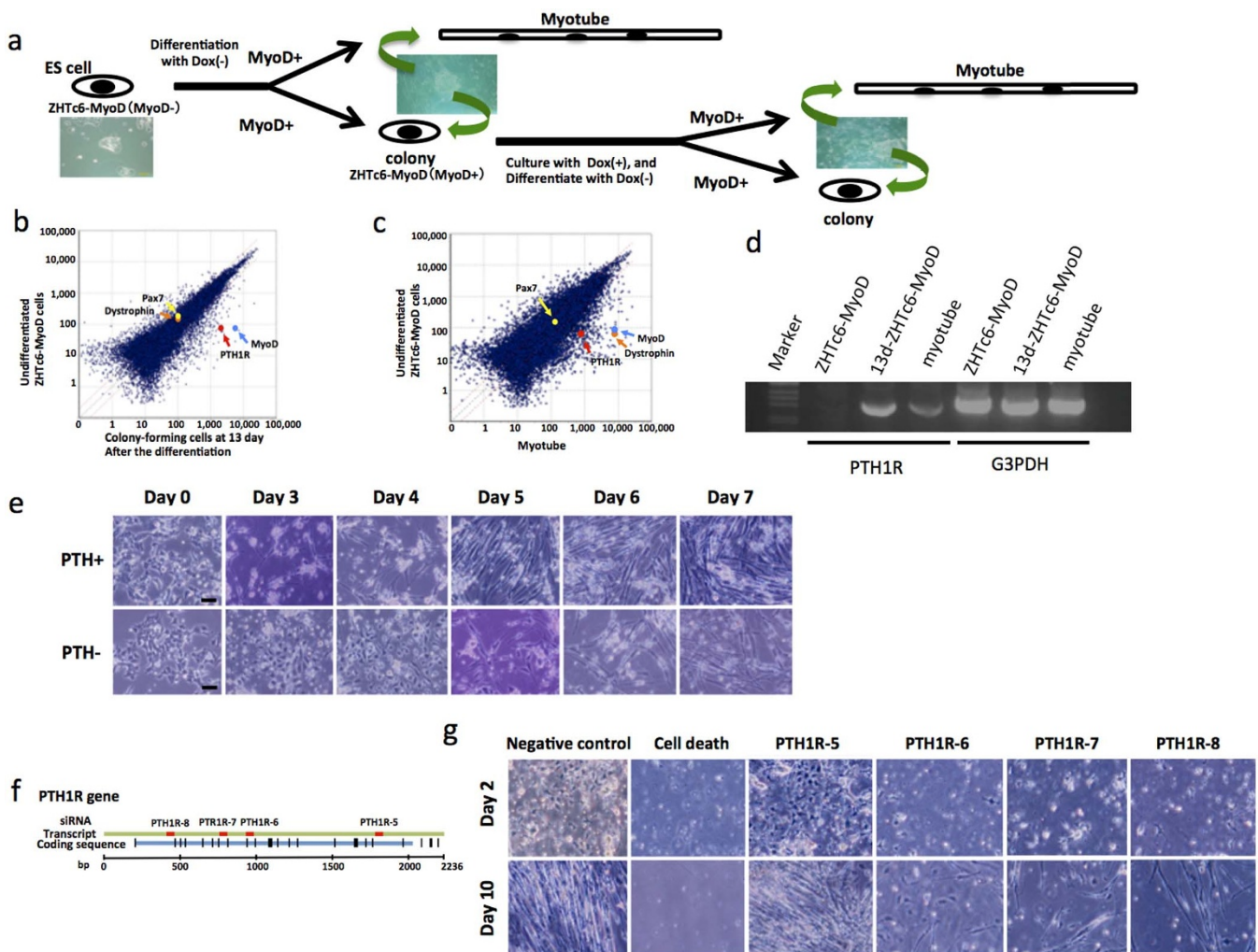


Figure 1 | ZHTc6-MyoD cell study. (a) Almost all of the ZHTc6-MyoD cells differentiated to form myotubes after the removal of Dox (-). However, a small fraction of the cells formed colonies. The colonies of the undifferentiated cells were cultured in maintenance medium, and subsequently differentiated into muscle lineage cells after the removal of Dox (-). (b) The DNA microarray analysis showed that MyoD expression in colony-forming cells at 13 days after differentiation was 90 times that in undifferentiated ZHTc6-MyoD cells. The levels of Pax7 and dystrophin expression were similar. PTH1R expression in the colony-forming cells at 13 days after differentiation was 40 times that in undifferentiated ZHTc6-MyoD cells. (c) PTH1R expression in the myotubes was 13 times that in undifferentiated ZHTc6-MyoD cells. (d) RT-PCR analysis also detected PTH1R expression in colony-forming cells at 13 days after differentiation (13d-ZHTc6-MyoD) and myotubes, but it was not expressed in the undifferentiated colonies. G3PDH expression was used as a positive control. Marker, DNA molecular weight Marker X (0.07–12.2 kb; Roche Mannheim, Germany). (e) The ZHTc6-MyoD cells that were cultured in differentiation medium containing PTH (PTH+) differentiated into spindle-shaped cells on day 3, and fused on day 4. The cells that were cultured in differentiation medium without PTH (PTH-) differentiated into spindle-shaped cells on approximately day 4, and fused on day 5. Scale bar represents 50 μ m. (f) The locations of PTH1R mRNA sequences to which the PTH1R siRNA 5 to 8 were complementary are indicated in the diagram. (g) Almost all of the cells transfected with the cell death control siRNA died. Most cells transfected with the PTH1R siRNA 6, 7, or 8 died on day 2. However, a few cells survived, and differentiated to myotubes on day 10. The cells transfected with PTH1R siRNA 5 survived, and differentiated in a manner similar to that observed for the negative control.

similar in both cell types. Dystrophin expression in the myotubes at 13 days after differentiation was also higher than that in undifferentiated ZHTc6-MyoD cells. We focused on parathyroid hormone receptor 1 (PTH1R) because its expression in the colony-forming cells at 13 days after differentiation was 40 times that in undifferentiated ZHTc6-MyoD cells (Fig. 1b). In addition, PTH1R expression in the myotubes was 13 times that in undifferentiated ZHTc6-MyoD cells (Fig. 1c).

Parathyroid hormone (PTH) has been shown to enhance the differentiation of mesoderm to various cell types, including chondrocytes, osteoclasts, cardiovascular cells, and smooth muscle cells^{16–19}. Skeletal muscle cells also differentiate from the mesoderm. Reverse transcription polymerase chain reaction (RT-PCR) analysis showed that PTH1R expression in the colony-forming cells after differenti-

ation was higher than that in myotubes. PTH1R expression was not detected in undifferentiated ZHTc6-MyoD cells (Fig. 1d). Therefore, we hypothesized that PTH is involved in myocyte differentiation.

The effect of PTH and PTH1R activation on ZHTc6-MyoD cell differentiation. To investigate the relationship between PTH and the differentiation of ZHTc6-MyoD cells, we compared the differentiation of ZHTc6-MyoD cells in the presence of the 34-residue amino-terminal fragment of PTH (PTH1-34; Sigma-Aldrich, St. Louis, MO, USA) to those cultured without PTH. The ZHTc6-MyoD cells were cultured in differentiation medium containing 20 nM PTH1-34 (PTH+). The control ZHTc6-MyoD cells were cultured in differentiation medium without PTH1-34 (PTH-; Fig. 1e). The PTH+ cells began to differentiate to spindle-shaped cells on day 3,

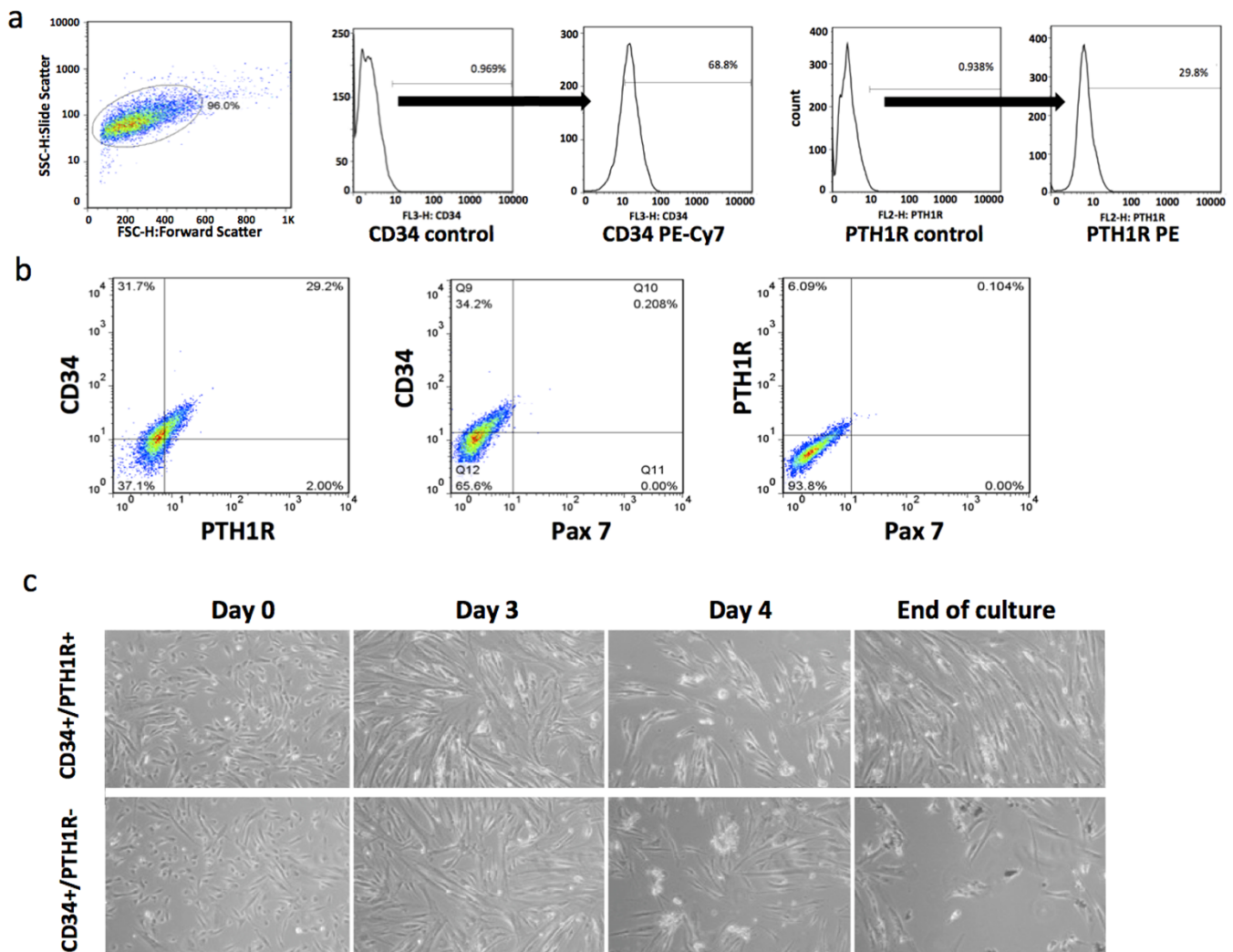


Figure 2 | FACS analysis and time-lapse imaging of human primary myogenic cells. (a) Human primary myogenic cells were isolated from biopsies collected from patients with DMD. Gating schematic for sorting and analyzing CD34 +/– and PTH1R +/– populations in the cells is shown in. FACS analysis revealed that 68.8% of cells were CD34+ and 29.6% were PTH1R+. Almost no Pax7+ cells were detected. CD34 and PTH1R controls represent unstained samples; CD34 PE-Cy7 and PTH1R PE represent the stained samples. (b) The two-parameter dot plot of CD34 PE-Cy7 and PTH1R PE signal intensities showed that 29.2% of the cells were both CD34+ and PTH1R+. (c) The time-lapse images of the CD34+/PTH1R+ cells and CD34+/PTH1R– cells were compared. The CD34+/PTH1R+ cells differentiated to form myosheets consisting of large multinucleated cells on day 3. The myosheets peeled off the plate on day 4. The CD34+/PTH1R+ cells continued to differentiate to myotubes, and became confluent on day 23, the endpoint of the experiment. In contrast, the CD34+/PTH1R– cells differentiated to poorly formed myotubes. A small number of the CD34+/PTH1R– cells differentiated to randomly moving, small round cells, but the myotubes that formed by day 26 (experiment endpoint) were not confluent.

and fused on day 4. In contrast, the PTH– cells differentiated to spindle-shaped cells on day 4, and fused on day 5. As cells differentiate, they become longer and fuse together. We counted the number of cells that were 150 μm or longer, thereby including the number of differentiated myotubes in the population. In order to quantitate the rate of differentiation in each of the two conditions (PTH+ and PTH–), we measured the ratio of long cells to the total number of cells (more than 300 cells in every measurement) every day for 7 days. The ratios (represented as a percentage) in the PTH– cells were 0%, 1%, 10.4%, 28.8%, 64.1%, and 93.1% on day 2, 3, 4, 5, 6, and 7, respectively. In contrast, the percentages of differentiated cells in PTH+ cells were 0%, 23.8%, 56.3%, 98.0%, 97.5%, and 97.9% on each of those days, respectively. Therefore, PTH accelerated the differentiation of the ZHTc6-MyoD ESCs to myotubes.

We subsequently investigated whether PTH1R is necessary for the differentiation of ZHTc6-MyoD cells. PTH1R expression in the differentiated cells was inhibited by 4 different PTH1R siRNA sequences (Fig. 1f). The Alexa-Fluor-488 (AF488) signal was

detected in almost all of the cells at two days after transfection with the AF488-labeled negative control siRNA (data not shown), and almost all the cells died after transfection with the cell-death control siRNA (Fig. 1g). Most of the cells died on day 2 following transfection with PTH1R siRNA 6, 7, or 8. However, a few of the PTH1R siRNA-transfected cells survived, and differentiated into myotubes on day 10. The PTH1R siRNA-5-transfected cells also survived, but differentiated in the same manner as the cells transfected with the negative control siRNA (Fig. 1g).

Fluorescence-activated cell sorting (FACS) analysis of human primary myogenic cells and the differentiation of sorted CD34+/PTH1R+ and CD34+/PTH1R– cells. We performed a FACS analysis (Fig. 2a and b) to determine the percentages of human primary myogenic cells that expressed PTH1R, Pax7, and the hematopoietic stem cell marker, CD34²⁰. Among the human primary myogenic cells isolated, 68.8% were CD34+ and 29.6% were PTH1R+ (Fig. 2a). The two-parameter dot plot of the CD34

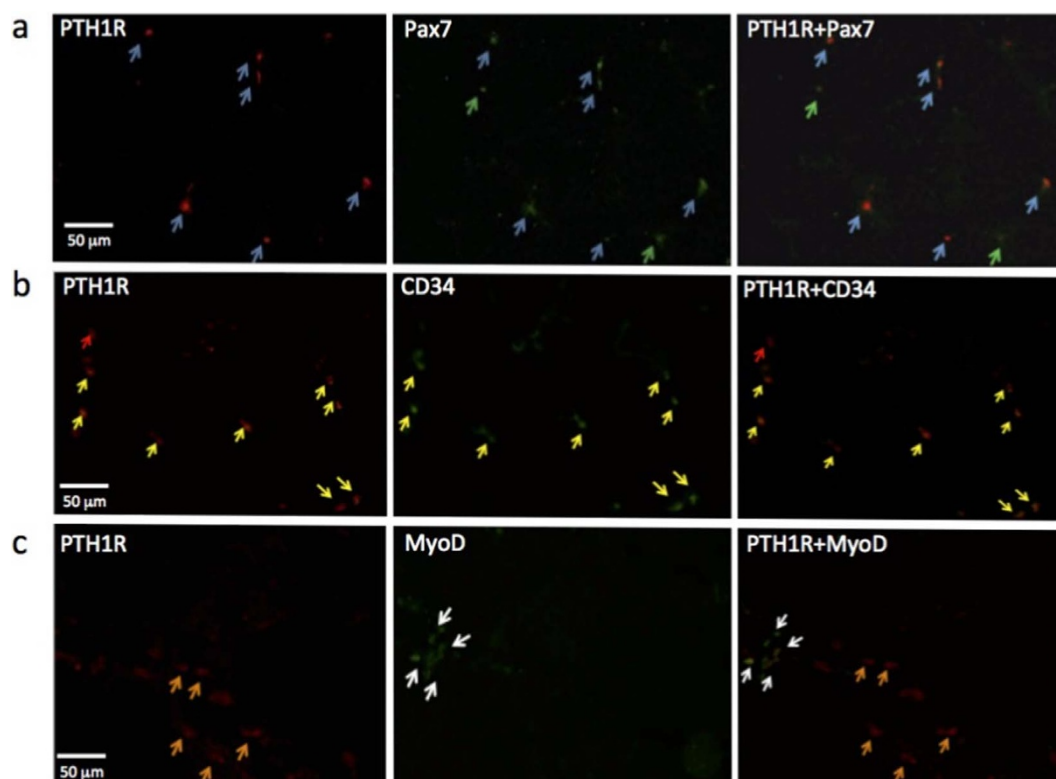


Figure 3 | Immunohistochemical staining for PTH1R, Pax7, CD34, and MyoD in mdx mice. (a) Double-labeled staining for Pax7 and PTH1R in mdx mice showed that almost all of the Pax7+ cells were PTH1R+, whereas a few cells were Pax7+ only. Blue arrow, PTH1R+/Pax7+ cell; Green arrow, PTH1R-/Pax7+ (b) Most of the PTH1R+ cells in the mdx mice were also CD 34+. A few cells were PTH1R+ only. Yellow arrow, PTH1R+/CD34+ cell; Red arrow, PTH1R+/CD34-. (c) Mdx cells that expressed both PTH1R and MyoD were not detected. Orange arrow, PTH1R+/MyoD- cell; White arrow, PTH1R-/MyoD+.

PE-Cy7 and PTH1R PE signals showed that 29.2% of the cells were both CD34+ and PTH1R+ (Fig. 2b), whereas Pax7+ cells were rarely detected.

Time-lapse imaging was used to compare the differentiation of the CD34+/PTH1R+ cells to that of the CD34+/PTH1R- cells (Supplementary Video 1, Fig. 2c). After the myocyte growth medium was replaced with differentiation medium containing 20 nM PTH 1-34, the cells began to differentiate, and formed myosheets²¹ consisting of large multinucleated cells on day 3. The myosheets peeled off the plate on day 4. The CD34+/PTH1R+ cells continued to differentiate to myotubes, and became confluent on day 23, which was the endpoint of the experiment. In contrast, the CD34+/PTH1R- cells differentiated to poorly formed myotubes that had not reached confluence by day 26 (experiment endpoint). In addition, a small number of the CD34+/PTH1R- cells differentiated to small, round, randomly moving cells. These findings indicate that PTH1R may be required for the differentiation of muscle stem cells.

PTH effect on immortalized human myogenic cells Hu5/KD3 (KD3). We also investigated the role of PTH in human myocyte differentiation. The immortalized human myogenic cell line, Hu5/KD3 (KD3), was cultured for 21 days in differentiation medium with and without 20 nM PTH1-34. The KD3 cells differentiated into myosheets, and began to beat on day 16 (Supplementary Video 2). The average numbers of beating myosheets in two 3.5-cm type I collagen-coated dishes in the PTH+ and PTH- groups were 26 and 4, respectively. In addition, the PTH+ cultures formed larger myosheets than those formed by the PTH- cells (data not shown). These results indicate that PTH is involved in myotube/myosheet formation and myosheet beating. However, similar experiments using C2C12 or human primary myogenic cells did not produce similar results.

Double-labeled immunohistochemical staining with PTH1R/Pax7, PTH1R/CD34, and PTH1R/MyoD. We investigated the expression of PTH1R in the skeletal muscle of mdx mice and patients with DMD. Double-labeled immunohistochemical staining of PTH1R/Pax7, PTH1R/CD34, and PTH1R/MyoD was performed to determine the stage of muscle differentiation. Almost all of the PTH1R+ cells from mdx mice were Pax7+, indicating they were satellite cells (Fig. 3a). A few Pax7+ cells did not express PTH1R. Almost all CD34+ cells in the mdx mice were PTH1R+ (Fig. 3b), with only a small fraction of PTH1R- cells observed. The PTH1R+ cells were highly similar, and did not express MyoD (Fig. 3c). Similar results were obtained in experiments using human skeletal muscle cells.

PTH administration improves muscle strength in mdx mice.

Four-week-old mdx mice were subcutaneously injected with 10, 60, or 200 $\mu\text{g}/\text{kg}/\text{d}$ of PTH or an equivalent volume of saline for 20 days to determine the optimal dose of PTH. The 60 $\mu\text{g}/\text{kg}/\text{d}$ dose was selected because the mice that received this dose had the longest hang time in the four-limb hanging wire test, and the histologic findings from the examination of their muscle tissue revealed improvement. The mdx mice that received 200 $\mu\text{g}/\text{kg}/\text{d}$ of PTH became hypercalcemic.

Six 4-week-old male mdx mice were subcutaneously injected with 60 $\mu\text{g}/\text{kg}/\text{d}$ of PTH for 59 days. Seven age-matched male mdx mice were injected with an equivalent volume of saline, and 6 age-matched male C57BL/10 wild-type mice with similar genetic backgrounds were used as normal controls. The four-limb hanging wire test was performed on day 10 (Fig. 4a). The mean hanging time for the PTH-treated mdx mice was 132 ± 61.6 s. In contrast, the mean hanging time for the saline-injected mdx mice ($n = 7$) was signifi-

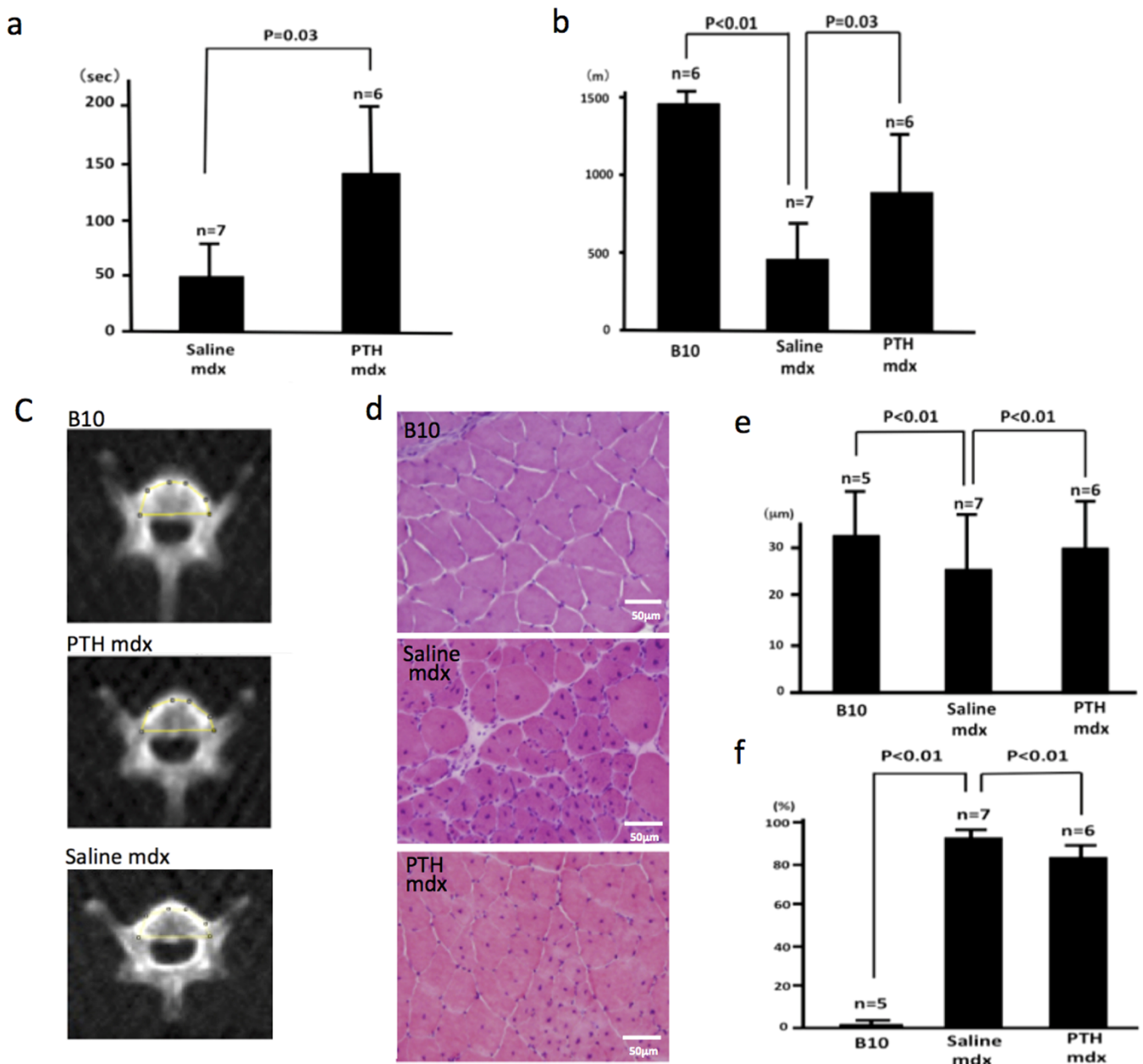


Figure 4 | *In vivo* analysis of the effect of PTH on muscle strength. (a) The mean hang time in the four-limb hanging wire test for the PTH-treated mdx mice ($n = 6$) was 132 ± 61.6 s. In contrast, the mean hang time for the saline-injected mdx mice ($n = 7$) was significantly shorter ($p = 0.03$) at 49.5 ± 44.9 s. (b) Mice were made to run on a treadmill at 25 cm/s for 100 min. All of the C57BL/10 mice ($n = 6$) ran for 100 min, and the mean distance covered was 1486 ± 7.4 m. The PTH-treated mdx ($n = 6$) mice ran a mean distance of 843.6 ± 352 m, but one did not run for 100 min. None of the saline-injected mdx mice ($n = 7$) ran for 100 min, and the mean distance covered was 425 ± 190 m. Both the C57BL/10- and PTH-treated mdx mice ran significantly longer than the saline-injected mdx mice ($p < 0.01$ and $p = 0.03$, respectively). (c) Mean mCT value of the fourth lumbar vertebrae of the mice in each group measured to confirm the effect of PTH on bone density. The mean mCT values of the C57BL/10, PTH-treated mdx, and saline-injected mdx mice were 1521.871, 1304.34, and 1207.272 Hounsfield units, respectively. (d) Thin sections of the gastrocnemius muscle from the C57BL/10, saline-injected mdx, and PTH-treated mdx mice were stained with HE for histological examination. (e) The diameters of myofibers in the tissues from the C57BL/10 ($n = 5$), saline-injected mdx ($n = 7$), and PTH-treated mdx ($n = 6$) mice were 33.62 ± 10.6 , 25.41 ± 10.4 , and 31.16 ± 12.9 μm , respectively ($p < 0.01$). (f) The rates of myofibers with central nuclei for the C57BL/10 ($n = 5$), saline-injected mdx ($n = 7$), and PTH-treated mdx ($n = 6$) mice were $0.34\% \pm 2.0\%$, $93.2\% \pm 2.0\%$, and $83.01\% \pm 4.0\%$, respectively ($p < 0.01$). These results show that the histology of myofibers from mdx mice is improved by PTH treatment. B10, C57BL/10; Saline mdx, saline-injected mdx; PTH mdx, PTH-treated mdx.

cantly shorter (49.5 ± 44.9 s; $p = 0.03$). The hanging times for all of the C57BL/10 mice were 5–6 s.

The treadmill test was performed on day 43. Mice were forced to run at a speed of 25 cm/s for 100 min on a treadmill with the belt parallel to the floor (Fig. 4b). The distance that they ran was recorded and compared. All of the C57BL/10 mice ($n = 6$) ran for 100 min,

with a mean distance of 1486 ± 7.4 m. The PTH-treated mdx mice ($n = 6$) ran a mean distance of 843.6 ± 352 m, and only one of the PTH-treated mice ran for 100 min. The saline-injected mdx mice ($n = 7$) ran a mean distance of 425 ± 190 m, and none of them ran for 100 min. Both the C57BL/10 and PTH-treated mdx mice ran significantly longer than the saline-injected mdx mice ($p < 0.01$



and $p = 0.03$, respectively). These results indicate that the PTH treatment significantly improved muscle strength in the mdx mice.

PTH administration improves bone density in mdx mice. Sixteen days after completing the treadmill test (day 59), a microcomputed tomography (mCT) scan of the fourth lumbar vertebra of each mouse in each group was recorded to assess the effect of PTH on bone structure. The mean mCT values of the C57BL/10, PTH-treated mdx, and saline-injected mdx mice were 1521.871, 1304.34, and 1207.272 Hounsfield units, respectively (Fig. 4c).

Serum creatine kinase and calcium level of mice after the administration of PTH. One day after mCT scanning was completed (day 60), all of the mice were sacrificed, and blood and tissue samples were collected for hematological and histological analyses. The creatine kinase (CK) levels were 1558.6 ± 1316.7 IU/L in the C57BL/10 mice ($n = 5$), 5508.8 ± 2149.7 IU/L in the PTH-treated mdx mice ($n = 6$), and 6630.1 ± 3811.2 IU/L in the saline-injected mdx mice ($n = 7$). The CK level in the C57BL/10 mice was clearly lower than that in the PTH- and saline-injected mdx mice ($p < 0.01$), and the CK levels of the PTH- and saline-injected mdx mice were statistically similar. The serum calcium levels of the C57BL/10 ($n = 5$), saline-injected mdx ($n = 7$), and PTH-treated mdx mice ($n = 6$) were 10.46 ± 1.461 , 9.871 ± 0.5233 , and 9.3833 ± 0.4845 mg/dL, respectively, all of which were statistically similar.

Histological changes in mdx mice treated with PTH. The histological analysis of the mdx mice revealed the destruction of massive groups of muscle fiber, followed by complete regeneration by 20 days of age, and the majority of the fibers contained central nuclei by the age of 12 weeks²². Nuclei were located at the periphery of the muscle fibers in the normal control mice. The mean diameters of the myofibers of the C57BL/10 ($n = 5$), saline-injected mdx ($n = 7$), and PTH-treated mdx mice ($n = 6$) at the age of approximately 13 (day 60) weeks were 33.62 ± 10.6 , 25.41 ± 10.4 , and 31.16 ± 12.9 μm , respectively ($p < 0.01$; Figs. 4d, 4e). The saline-injected mdx mice had smaller, more rounded fibers (regenerative fibers) than the PTH-treated mdx mice. The percentage of myofibers with central nuclei in the C57BL/10 ($n = 5$), saline-injected mdx ($n = 7$), and PTH-treated mdx mice ($n = 6$) were $0.34\% \pm 0.2\%$, $93.2\% \pm 2.0\%$, and $83.01\% \pm 4.0\%$, respectively ($p < 0.01$; Fig. 4d and f). These results indicated that the PTH treatment significantly improved the structure of muscle fibers in the mdx mice. We, therefore, concluded that PTH treatment improved muscle weakness by enhancing muscle fiber regeneration.

Discussion

A peptide hormone secreted by the parathyroid glands, PTH, acts primarily on bone and kidney cells, and is involved in systemic calcium regulation^{17,23}. In the kidney, PTH1R is most often detected in the basolateral region of the plasma membrane of epithelial cells in the proximal and distal renal tubules. In bone, PTH1R is expressed on the plasma membrane of osteocytes, osteoblasts, and other mesenchyme-derived cells^{24,25}. PTH1R is also expressed by cells in the gut and in a number of neoplastic tissues, including colorectal carcinoma, prostate cancer, renal cell carcinoma, and osteosarcoma²⁶.

Parathyroid hormone-related protein (PTHrP) also binds to the PTH1R^{16,27,28}. In mature animals, PTH1R and PTHrP are abundantly expressed throughout the cardiovascular system, including vascular smooth muscle and endothelial cells, where PTHrP regulates the proliferation of vascular smooth muscle cells¹⁹. PTH promotes cardiac repair by enhancing cell survival in the ischemic heart and stimulating neovascularization following myocardial infarction¹⁸. These findings collectively indicate that PTH is involved in the differentiation of vascular smooth muscle cells. Like kidney and bone tissue, vascular smooth muscle and skeletal muscle cells are derived

from the mesoderm. Thus, PTH may also influence the differentiation of skeletal muscle cells.

The transfection of ZHTc6-MyoD cells with PTH1R siRNA 6, 7, or 8 inhibited differentiation. These results revealed that PTH1R is necessary for the differentiation of ZHTc6-MyoD cells to myotubes. Only 1 out of the 4 siRNA sequences tested (siRNA 5) appears to have failed to inhibit the expression of PTH1R. The failure of this one assay may have been due to the complementarity of the siRNA to the cDNA encoding the C-terminal region of the PTH1R protein. It is important to note that the efficacy of these siRNA molecules are neither tested nor guaranteed by the manufacturer and that the sequences are merely a product of bioinformatics algorithms. Therefore, given the success of the majority of the siRNA assays (3 out of 4 unique siRNA sequences) in knocking down PTH1R, and the failure of these cells to differentiate, we safely conclude that PTH1R is necessary for the differentiation of ZHTc6-MyoD cells to myotubes.

In a previous study, the embryos of PTH1R ($-/-$) knockout mice were smaller than those of control mice as early as embryonic day (E) 9.5²⁹, but the histological evaluation showed diminished organ size only, with no other gross developmental defects. Although the number of PTH1R ($-/-$) embryos appeared to meet Mendelian expectations at E9.5, all of the embryos were dead by E14.5. By E13, the myoblasts in the healthy control animals actively proliferated, and somite muscle fibrils were observed on E14.5³⁰. Thus, the death of the PTH1R knockout embryos coincided with the period during which mesoderm-derived muscle cells differentiate.

In our current study, PTH accelerated the differentiation of ZHTc6-MyoD cells to a myocyte lineage. The CD34+/PTH1R+ cells sorted from human primary myogenic cells differentiated to myotubes, and reached confluence. In contrast, the myotubes formed by the CD34+/PTH1R- cells did not reach confluence. Our experiments using KD3 cells also indicated that PTH is involved in myotube/myosheet formation and myosheet beating. Therefore, we concluded that the interaction between PTH and PTH1R contributes to muscle differentiation.

Our immunohistochemical analysis of mouse and human skeletal muscle showed that nearly all of the PTH1R+ cells were Pax7+, CD34+, and MyoD-. Pax7+/MyoD+ expression by myoblasts is a biomarker of active proliferation³¹. Thus, our results suggests that the PTH1R+ cells more closely resembled muscle stem cells than activated satellite cells, such as quiescent satellite cells. Therefore, PTH1R is a possible biomarker for satellite cells in skeletal muscle. Furthermore, PTH1R expression was detected not only in the colony-forming cells (at 13 days) and muscle stem cells in human and mouse tissues, but also in myotubes.

This observation suggests that the activation of PTH1R might act as a trigger for differentiation of stem cells into the muscle lineage and may therefore also relate to myoblast fusion. Further experiments, however, are needed to prove this hypothesis.

The reason for our inability to detect Pax7+ cells in our FACS analysis is unclear, and future experiments investigating Pax7 expression during the differentiation of muscle cells are warranted to clarify our findings.

The four-limb hanging wire test and the treadmill test revealed that the PTH treatment significantly improved the muscle strength of mdx mice. The histological characteristics of the skeletal muscle of the mdx mice also improved following PTH treatment. However, CK, which is a biomarker of myofiber damage, did not decrease, indicating that the stability of the membrane did not improve. Thus, the PTH-mediated increase in muscle strength in mdx mice was probably the result of more rapid muscle regeneration, compared to the non-treated mdx mice.

Rufo et al. reported that mCT revealed reduced bone mass in mdx mice compared with wild-type mice³². Other previous studies also showed that reduced bone mass in mdx mice improved following PTH treatment^{32,33}. In our current study, the mean mCT values of the



fourth lumbar vertebra of the mdx mice increased following PTH treatment, suggesting that PTH enhances ossification in dystrophin-deficient mice. Our results collectively indicate that PTH1R and PTH are important factors in skeletal muscle fiber differentiation. The increased rate of myocyte regeneration in mdx mice following PTH treatment suggests that PTH might represent an effective treatment for patients with degenerative muscle diseases, such as DMD.

Methods

Cell culture and PTH treatment of C2C12 and ZHTc6-MyoD mouse myoblasts.

The ZHTc6-MyoD cells were grown in maintenance medium, as previously described³⁴. The maintenance medium contained leukemia inhibitory factor (Life Technologies, Carlsbad, CA, USA), Dox (Takara Bio, Shiga, Japan), and 15% Knockout SR (Life Technologies). To induce the differentiation of the ZHTc6-MyoD cells, the maintenance medium was replaced with a differentiation medium, which lacked leukemia inhibitory factor (Invitrogen, CA, USA) and Dox (Takara Bio Inc., Shiga, Japan) and contained 4% fetal bovine serum (FBS; Life Technologies) instead of 15% Knockout SR (Invitrogen). The C2C12 mouse myoblast cells were propagated in growth medium, which consisted of Dulbecco's modified Eagle's medium (DMEM; Invitrogen) containing 10% FBS and 1% Antibiotic-Antimycotic solution (Life Technologies). To induce the differentiation of the C2C12 cells, the growth medium was replaced with differentiation medium, which consisted of DMEM containing 2% horse serum (Life Technologies), 1% Insulin-Transferrin-Selenium-A (Life Technologies), and 1% Antibiotic-Antimycotic solution. The C2C12 cells were cultured in type I collagen-coated culture dishes (Iwaki, Tokyo, Japan). To test the effect of PTH, differentiation was induced using differentiation medium supplemented with 20 nM rat PTH1-34³⁵, and the medium was replenished every 2–3 days. Differentiation medium without PTH 1-34 was used for the control cells.

Cell culture of immortalized human myogenic cell clone Hu5/KD3. The human Hu5/KD3 myogenic cell line was kindly provided by Dr. Naohiro Hashimoto Naohiro of the National Center for Geriatrics and Gerontology (Obu, Japan). The Hu5/KD3 cells were maintained in myocyte growth medium (pmGM), which consisted of DMEM containing 20% FBS, 2% Ultrosor G (Biosepra, Cedex-Saint-Christophe, France), and 1% Antibiotic-Antimycotic solution in type I collagen-coated dishes (Iwaki) at 37°C in a 5% CO₂ atmosphere. Myogenic differentiation was induced by replacing the pmGM with primary myocyte differentiation medium (pmDM), which consisted of DMEM containing 2% horse serum and Insulin-Transferrin-Selenium-A, as described previously³⁶. The effect of PTH on the differentiation of Hu5/KD3 cells was performed using the procedure described above for the C2C12 and ZHTc6-MyoD cells using pmDM containing 20 nM human PTH1-34.

Isolation and culture of human primary myogenic cells. Tissue was biopsied from the biceps brachii of patients with DMD who provided informed consent prior to the procedure. The muscle tissue was minced before incubation in 5 mL TrypLE Express (Life Technologies) for 5 min at room temperature, and centrifuged at 200 rpm for 2 min. The supernatant was transferred to another tube, and 1 ml of FBS was added. The above-mentioned incubation was repeated, and the collected supernatant was centrifuged at 1000 rpm for 10 min. The supernatant was discarded, and the cell pellet was suspended in pmGM. The cell suspension was spread onto a type I collagen-coated dish. Colonies were visible after approximately 10 days. The cells were detached from the plate with trypsin (Life Technologies), and cultured in pmGM. Myogenic differentiation was induced by replacing the pmGM with pmDM, as previously described³⁷.

cDNA microarray analysis. The undifferentiated ZHTc6-MyoD cells were collected by centrifugation after trypsin treatment. To collect the colony-forming cells at 13 days after differentiation, the ZHTc6-MyoD cells were cultured in the differentiation medium for 13 days. The myotubes in the dish were subsequently removed from the plates by flushing with the medium, and the colonies were collected by centrifugation after trypsin treatment. The differentiation medium for the myotubes was replenished with fresh differentiation medium containing 2 μM ganciclovir (Sigma-Aldrich) at 3 days post-differentiation to remove undifferentiated ZHTc6-MyoD cells, and the cells were cultured for an additional 10 days³⁴. Total RNA was isolated from undifferentiated ZHTc6-MyoD cells, colony-forming cells at 13 days after differentiation, and myotubes using the ISOGEN solution (Nippon Gene, Tokyo, Japan), according to the manufacturer's instructions. The RNAs were reverse transcribed in the presence of Cy3- or Cy5-labeled cytidine triphosphate. The labeled cDNAs were hybridized to a Filgen Array Mouse 32K microarray (Oxford Gene Technology, Oxford, UK) that contained 31 769 genes, and the signals were detected using a GenePix 4000B array scanner (Molecular Devices, Sunnyvale, CA, USA) commissioned to Filgen (Aichi, Japan).

siRNA-mediated knock down of PTH expression. Four different of siRNA sequences, Mm-Pthr1-5, Mm-Pthr1-6, Mm-Pthr1-7, and Mm-Pthr1-8 (Qiagen, Hilden, Germany), were used to inhibit the expression of PTH1R in ZHTc6-MyoD cells during differentiation. AllStars Mm/Rn Cell Death Control siRNA (Qiagen) was used for the cell death control, and AllStars Neg siRNA AF488 (Qiagen) was used for a

negative control. The differentiation of the ZHTc6-MyoD cells was induced 2 days before transfection. A total of 5×10^5 cells were seeded in a 6-well type I collagen-coated plate. The cells were incubated for a short time and transfected with 3000 ng siRNA using the HiPerFect transfection reagent (Qiagen), according to the manufacturer's instructions. The differentiation medium was replenished at 48 h post-transfection.

FACS analysis. The human myogenic cells were isolated, as previously described³⁵. The FACS analysis was performed using goat anti-Pax7 (LifeSpan BioSciences, Seattle, WA, USA), rabbit anti-PTH1R (Sigma-Aldrich), and PE-Cy7-labeled anti-human CD34 (BioLegend, San Diego, CA, USA) primary antibodies. Alexa-Fluor-488-labeled donkey anti-goat IgG (Life Technologies) and PE-labeled donkey anti-rabbit IgG (eBioscience, San Diego, CA, USA) antibodies were used as secondary antibodies for Pax7 and PTH1R detection, respectively. Flow cytometry and cell sorting were performed using a BD FACSVantage SE flow cytometer (BD Bioscience, San Jose, CA, USA) commissioned to ReproCell (Kanagawa, Japan).

Time-lapse recording. Time-lapse images were recorded every 30 min using a Cell watcher plus (Corefront, Tokyo, Japan).

RT-PCR analysis. Total RNA was isolated from cells using the Trizol reagent (Life Technologies), according to the manufacturer's protocol. The SuperScript First-Strand Synthesis System (Life Technologies) and random primers were used for first-strand cDNA synthesis. RT-PCR was performed with the following primers as previously described, using the glyceraldehyde-3-phosphate dehydrogenase (G3PDH) transcript as a positive control: PTH1R-F, 5'-AGGTGGTCCAGGG-CACAA-3'; PTH1R-R, 5'-CAACTTTCCTCCGTGAGGC-3'; Pax7-F, 5'-ACCGAGTGCCTCAGAAATCAA-3'; Pax7-R, 5'-TCCTCTCGAAAGCCTTCTCC-3'; G3PDH-F, 5'-TCCATGACAACTTTGGCATCGTGG-3'; and G3PDH-R, 5'-GTTGCTGTTGAAGTCACAGGAGAC-3'^{38–40}. Thermal cycling was performed using an initial denaturation at 96°C for 5 min, followed by 30 cycles of 94°C for 1 min, 55°C for 1 min, and 72°C for 5 min, with a final incubation at 72°C for 10 min.

Four-limb hanging wire test and treadmill test. All of our animal experiments were approved by the ethics committee of the Center for Animal Resources and Development, Kumamoto University, Japan, and were carried out in accordance with the approved guidelines. Mdx mice were treated with subcutaneous injections of rat PTH 1-34 or saline. For the hanging wire test, the mice were placed in a prone position on a wire grid, and the grid was inverted above a cage (O'Hara & Co, Tokyo, Japan). A 2.8-g weight was attached to the tail of each mouse to allow greater distinction between higher levels of strength. The hanging wire test was performed 3 times for each mouse, and the longest hanging time was used for the data analysis⁴¹. The treadmill test was performed using an LE8710 treadmill (Panlab, Barcelona, Spain), as previously described⁴².

Histological and immunohistochemical analyses. Human muscle biopsy specimens were obtained as described above. Samples of the gastrocnemius were collected from C57BL/10 and mdx mice following euthanization, and the tissues were cryosectioned. Hematoxylin and eosin (HE) staining was performed for the myofiber analysis. Rabbit anti-PTH1R (1 : 400; Sigma-Aldrich), goat anti-Pax7 (1 : 300; LifeSpan Bioscience), goat anti-CD34 (1 : 100; Santa Cruz Biotechnologies, Dallas, TX, USA), and goat anti-MyoD (1 : 100; Santa Cruz Biotechnologies) monoclonal antibodies were used as primary antibodies for immunohistochemical staining. Primary antibody reactivity was detected using an Alexa-Fluor-555-labeled anti-rabbit IgG (Life Technologies) or an Alexa-Fluor-488-labeled anti-goat IgG secondary antibody. The slides were examined using fluorescence microscopy.

Muscle fiber size and central nucleus analysis. The smallest cross-sectional diameter of the myofibers and the number of central nuclei in the myofibers (>500 fibers per animal) were determined using the Image J (NIH, Bethesda, MD, USA) and Cell Sense (Olympus, Tokyo, Japan) software suites, respectively, based on the analysis of digital images of the HE stained sections. Statistical analyses of the fiber size and central nuclei data were performed using the Microsoft Excel, version 14.2.5, software (Redmond, WA, USA).

Serum CK and Ca. The serum CK and Ca levels were measured using the Fuji Dri-Chem system (Fuji Film Medical, Tokyo, Japan), according to the manufacturer's instructions.

Bone density analysis using Mct. High-resolution X-ray microcomputed tomography (mCT) of the fourth lumbar vertebra was performed using a FLEX Triumph CT scanner (TriFoil Imaging, Northridge, CA, USA) operated at 40 kV and 790 mA. The X-ray transmission images were acquired using 256 projections over 360 degrees, a 256-ms exposure/projection, $\times 2$ magnification, and a focal spot of 84 μm. The geometrical field of view was 59×59 mm for a 512×512 matrix. Each 512-slice mCT image set was reconstructed using a 115-μm pixel size to generate the three-dimensional images. The mCT value of the lumbar vertebral body (mean density within the yellow line) was measured using the Image J software.

Statistical analysis. Microsoft Excel was used to perform the statistical analysis. Student *t*-tests were used to identify significant differences between groups. Results of



comparisons with $p < 0.05$ were considered to represent statistically significant differences.

- Koenig, M. *et al.* Complete cloning of the Duchenne muscular dystrophy (DMD) cDNA and preliminary genomic organization of the DMD gene in normal and affected individuals. *Cell* **50**, 509–517 (1987).
- Nelson, S. F., Crosbie, R. H., Miceli, M. C. & Spencer, M. J. Emerging genetic therapies to treat Duchenne muscular dystrophy. *Curr. Opin. Neurol.* **22**, 532–538 (2009).
- Goemans, N. M. *et al.* Systemic administration of PRO051 in Duchenne's muscular dystrophy. *N. Engl. J. Med.* **364**, 1513–1522 (2011).
- Ozasa, S. *et al.* Efficient conversion of ES cells into myogenic lineage using the gene-inducible system. *Biochem. Biophys. Res. Co.* **357**, 957–963 (2007).
- Yoshida, N. *et al.* Cell heterogeneity upon myogenic differentiation: down-regulation of MyoD and Myf-5 generates 'reserve cells'. *J. Cell Sci.* **111**, 769–779 (1998).
- Mauro, A. Satellite cell of skeletal muscle fibers. *J. Biophys. Biochem. Cy.* **9**, 493–495 (1961).
- Seale, P. *et al.* Pax7 is required for the specification of myogenic satellite cells. *Cell* **102**, 777–786 (2000).
- Rooney, J. E., Gurbur, P. B., Yablonska-Reuveni, Z. & Burkin, D. J. Laminin-111 restores regenerative capacity in a mouse model for alpha7 integrin congenital myopathy. *Am. J. Pathol.* **174**, 256–264 (2009).
- Beauchamp, J. R. *et al.* Expression of CD34 and Myf5 defines the majority of quiescent adult skeletal muscle satellite cells. *J. Cell Biol.* **151**, 1221–1234 (2000).
- Covault, J. & Sanes, J. R. Distribution of N-CAM in synaptic and extrasynaptic portions of developing and adult skeletal muscle. *J. Cell Biol.* **102**, 716–730 (1986).
- Ratajczak, M. Z. *et al.* Expression of functional CXCR4 by muscle satellite cells and secretion of SDF-1 by muscle-derived fibroblasts is associated with the presence of both muscle progenitors in bone marrow and hematopoietic stem/progenitor cells in muscles. *Stem Cells* **21**, 363–371 (2003).
- Wozniak, A. C. *et al.* C-Met expression and mechanical activation of satellite cells on cultured muscle fibers. *J. Histochem. Cytochem.* **51**, 1437–1445 (2003).
- Moss, F. P. & Leblond, C. P. Satellite cells as the source of nuclei in muscles of growing rats. *Anat. Rec.* **170**, 421–435 (1971).
- Bischoff, R. Regeneration of single skeletal muscle fibers in vitro. *Anat. Rec.* **182**, 215–235 (1975).
- Campion, D. R. The muscle satellite cell: a review. *Int. Rev. Cytol.* **87**, 225–251 (1984).
- Mannstadt, M., Juppner, H. & Gardella, T. J. Receptors for PTH and PTHrP: their biological importance and functional properties. *Am. J. Physiol.* **277**, F665–F675 (1999).
- Blair, H. C., Sun, L. & Kohanski, R. A. Balanced regulation of proliferation, growth, differentiation, and degradation in skeletal cells. *Ann. N.Y. Acad. Sci.* **1116**, 165–73 (2007).
- Huber, B. C. *et al.* Comparison of parathyroid hormone and G-CSF treatment after myocardial infarction on perfusion and stem cell homing. *Am. J. Physiol. Heart C.* **298**, H1466–1471 (2010).
- Song, G. J., Fiaschi-Taesch, N. & Bisello, A. Endogenous parathyroid hormone-related protein regulates the expression of PTH type 1 receptor and proliferation of vascular smooth muscle cells. *Mol. Endocrinol.* **23**, 1681–1690 (2009).
- Goodell, M. A. *et al.* Dye efflux studies suggest that hematopoietic stem cells expressing low or undetectable levels of CD34 antigen exist in multiple species. *Nat. Med.* **3**, 1337–1345 (1997).
- Mukai, A. & Hashimoto, N. Localized cyclic AMP-dependent protein kinase activity is required for myogenic cell fusion. *Exp. Cell Res.* **314**, 387–397 (2008).
- Tanabe, Y., Esaki, K. & Nomura, T. Skeletal muscle pathology in X chromosome-linked muscular dystrophy (mdx) mouse. *Acta Neuropathol.* **69**, 91–95 (1986).
- Shimizu, E., Selvamurugan, N., Westendorf, J. J. & Partridge, N. C. Parathyroid hormone regulates histone deacetylases in osteoblasts. *Ann. N.Y. Acad. Sci.* **1116**, 349–353 (2007).
- Jacome-Galarza, C. E., Lee, S. K., Lorenzo, J. A. & Aguila, H. L. Parathyroid hormone regulates the distribution and osteoclastogenic potential of hematopoietic progenitors in the bone marrow. *J. Bone Miner. Res.* **26**, 1207–1216 (2011).
- Esbrit, P. & Alcaraz, M. J. Current perspectives on parathyroid hormone (PTH) and PTH-related protein (PTHrP) as bone anabolic therapies. *Biochem. Pharmacol.* **85**, 1417–1423 (2013).
- Lupp, A. *et al.* Immunohistochemical identification of the PTH1R parathyroid hormone receptor in normal and neoplastic human tissues. *Eur. J. Endocrinol.* **162**, 979–986 (2010).
- Schluter, K. D. & Piper, H. M. Cardiovascular actions of parathyroid hormone and parathyroid hormone-related peptide. *Cardiovasc. Res.* **37**, 34–41 (1998).
- Philbrick, W. M. *et al.* Defining the roles of parathyroid hormone-related protein in normal physiology. *Physiol. Rev.* **76**, 127–173 (1996).
- Lanske, B. *et al.* PTH/PTHrP receptor in early development and Indian hedgehog-regulated bone growth. *Science* **273**, 663–666 (1996).
- Rugh, R. The mouse. (Oxford University press, Oxford; 1994).
- Wen, Y. *et al.* Constitutive Notch activation upregulates Pax7 and promotes the self-renewal of skeletal muscle satellite cells. *Mol. Cell Biol.* **32**, 2300–2311 (2012).
- Rufo, A. *et al.* Mechanisms inducing low bone density in Duchenne muscular dystrophy in mice and humans. *J. Bone Miner. Res.* **26**, 1891–1903 (2011).
- Gray, S. K. *et al.* Black bear parathyroid hormone has greater anabolic effects on trabecular bone in dystrophin-deficient mice than in wild type mice. *Bone* **51**, 578–585 (2012).
- Niwa, H., Miyazaki, J. & Smith, A. G. Quantitative expression of Oct-3/4 defines differentiation, dedifferentiation or self-renewal of ES cells. *Nat. Genet.* **24**, 372–376 (2000).
- Guo, J. *et al.* Signal-selectivity of parathyroid hormone (PTH)/PTH-related peptide receptor-mediated regulation of differentiation in conditionally immortalized growth-plate chondrocytes. *Endocrinology* **142**, 1260–1268 (2001).
- Hashimoto, N. *et al.* Immortalization of human myogenic progenitor cell clone retaining multipotentiality. *Biochem. Biophys. Res. Co.* **348**, 1383–1388 (2006).
- Wada, M. R., Inagawa-Ogashiwa, M., Shimizu, S., Yasumoto, S. & Hashimoto, N. Generation of different fates from multipotent muscle stem cells. *Development* **129**, 2987–2995 (2002).
- Kuwahara, M. *et al.* Expression of bone type 1 PTH receptor in rats with chronic renal failure. *Clin. Exp. Nephrol.* **11**, 34–40 (2007).
- Grefte, S., Kuijpers, M. A., Kuijpers-Jagtman, A. M., Torensma, R. & Von den Hoff, J. W. Myogenic capacity of muscle progenitor cells from head and limb muscles. *Eur. J. Oral. Sci.* **120**, 38–45 (2012).
- Kimura, S. *et al.* Novel mutation in splicing donor of dystrophin gene first exon in a patient with dilated cardiomyopathy but no clinical signs of skeletal myopathy. *J. Child Neurol.* **22**, 901–906 (2007).
- Van Putten, M. *et al.* A 3 months mild functional test regime does not affect disease parameters in young mdx mice. *Neuromuscular Disord.* **20**, 273–280 (2010).
- Aoki, Y. *et al.* Bodywide skipping of exons 45–55 in dystrophic mdx52 mice by systemic antisense delivery. *Proc. Natl. Acad. Sci. U.S.A.* **109**, 13763–13768 (2012).

Acknowledgments

We thank S. Nakano and K. Goto at Kumamoto University Graduate School for their assistance with animal care and mCT analysis, respectively. This study was supported by research grants from the Ministry of Health, Labor, and Welfare (grant no. 22-5) and the Ministry of Education, Culture, Sports, Science, and Technology (grant no. 24615005), Japan.

Author contributions

S.K. designed and executed the experiments, and wrote the manuscript. K.Y. performed the histological studies and immunohistochemical staining.

Additional information

Supplementary information accompanies this paper at <http://www.nature.com/scientificreports>

Competing financial interests: The authors declare no competing financial interests.

How to cite this article: Kimura, S. & Yoshioka, K. Parathyroid hormone and parathyroid hormone type-1 receptor accelerate myocyte differentiation. *Sci. Rep.* **4**, 5066; DOI:10.1038/srep05066 (2014).



This work is licensed under a Creative Commons Attribution-NonCommercial-NoDerivs 3.0 Unported License. The images in this article are included in the article's Creative Commons license, unless indicated otherwise in the image credit; if the image is not included under the Creative Commons license, users will need to obtain permission from the license holder in order to reproduce the image. To view a copy of this license, visit <http://creativecommons.org/licenses/by-nc-nd/3.0/>